Global Comparison of Benthic Nepheloid Layers Based on 52 years of Nephelometer and Transmissometer Measurements

*Wilford D. Gardner[a]
[a] Texas A&M University
College Station, TX 77843
USA
wgardner@ocean.tamu.edu

Mary Jo Richardson[b]
[b] Department of Oceanography
Texas A&M University
College Station, TX 77843
USA
mrichardson@ocean.tamu.edu

Alexey V. Mishonov[c]
[c] Cooperative Institute for Climate and Satellites (CICS-MD), University of Maryland
National Centers for Environmental Information (NCEI), NOAA affiliate
Silver Spring, MD 20910
USA
alexey.mishonov@noaa.gov

Pierre E. Biscaye[d]
[d] Lamont-Doherty Earth Observatory of Columbia University
Palisades, NY 10964
USA
biscaye@ldeo.columbia.edu

*Corresponding author: wgardner@ocean.tamu.edu

Abstract

Global maps of maximum bottom particle concentration, benthic nepheloid layer thickness, and integrated particle mass in benthic nepheloid layers (BNL) based on 2412 global profiles collected using the Lamont Thorndike nephelometer from 1964-1984 are compared with maps of those same properties compiled from 6,392 global profiles measured by transmissometers from 1979 to 2016. Outputs from both instruments were converted to particulate matter concentration (PM). The purposes of this paper are to compare global differences and similarities in the location and intensity of BNLs measured with these two independent instruments over slightly overlapping decadal time periods, to combine the data sets in order to expand the time scale of global in situ measurements of BNLs, and to gain insight about the factors creating/sustaining BNLs. The similarity between general locations of high and low particle concentration BNLs during the two time periods indicates that the driving forces of erosion and resuspension of bottom sediments are spatially persistent during recent decadal time spans, though in areas of strong BNLs, intensity is highly episodic. Topography and well-developed current systems play a role. These maps will help to understand deep ocean sediment dynamics, linkage with upper ocean dynamics, the potential for scavenging of adsorption-prone elements near the seafloor, and provide a comprehensive comparison of these data sets on a global scale.

During both time periods, BNLs are weak or absent in most of the Pacific, Indian, and Atlantic basins away from continental margins. High surface eddy kinetic energy is associated with the Kuroshio Current east of Japan. Both data sets show weak BNLs south of the Kuroshio, but no transmissometer data have been collected beneath the

Kuroshio itself. Sparse nephelometer data show moderate BNLs just north of the Kuroshio Extension, but with much lower concentrations than beneath the Gulf Stream. Strong BNLs are found in areas where eddy kinetic energy in overlying waters, mean kinetic energy near bottom, and energy dissipation within the bottom boundary layer are high. Areas of strongest BNLs include the Western North Atlantic, Argentine Basin (South Atlantic), areas around South Africa tied to the Agulhas Current region, and somewhat random locations in the Antarctic Circumpolar Current of the Southern Ocean.

1. Introduction

Optical instruments measuring forward scattering (referred to here as nephelometers) have been used for many decades to estimate particle abundance and distribution in bodies of water (Jerlov, 1953; Thorndike, 1975; Biscaye and Eittreim, 1977). In the 1970's, transmissometers were developed to measure the attenuation of light across a known path length to estimate particle concentration (Bartz et al., 1978). Numerous papers have been written using data from these, and similar instruments. Two multi decades-long global data sets have been collected: first using the Lamont Thorndike nephelometer (1960-1984; Thorndike, 1975) and second, using the SeaTech and WetLabs transmissometers (1979-2016; Gardner et al., 2018a, b). During a 1979 expedition of R/V *Knorr* (KN74), both instruments were used simultaneously in profiling and bottom-moored configurations and compared well in predicting particle concentrations (Gardner et al., 1985). We now combine those global data sets to quantify and compare benthic nepheloid layer (BNL) characteristics and location in the ocean over the last 52 years.

It is well known that particles in the euphotic zone of the open ocean result mainly from primary production of phytoplankton. Phytoplankton and phytodetritus are grazed by zooplankton, pelletized or aggregated into marine snow and rapidly remineralized during sinking (Honjo et al., 2008), processes that quickly reduce the particle concentration with depth. Once particles reach the seafloor they are incorporated into the bottom sediments.

Optical and filtration measurements have shown that although particle concentrations in the open ocean decrease to very low minimum values in the water column deeper than 100-200 m (5-12 $\mu g\ l^{-1}$; Biscaye and Eittreim, 1974; Brewer et al., 1976; Gardner et al., 1985), particle concentration can increase near the seafloor, indicating either erosion and resuspension due to bottom currents (Biscaye and Eittreim, 1974), or inhibited settling through bottom boundary layer turbulent mixing. The geographic variability of particle concentrations near the seafloor is orders of magnitude greater than in the mid-water column, sometimes reaching 100's-1000's $\mu g\ l^{-1}$ (Biscaye and Eittreim, 1974; 1977; Hill et al., 2011; Hayes et al., 2015b; Gardner et al., 2017; 2018a). High-resolution vertical measurements through the entire water column collected primarily during CTD hydrocasts with attached optical sensors, allows detection of BNLs. Profiling floats and gliders equipped with optical sensors have increased temporal and spatial coverage (Johnson et al, 2009), however most floats or gliders presently profile to 2000 m or less. Gliders that will profile to 6000 m are being built. We have yet to see how close to the seafloor they can safely make measurements. Therefore, these two data sets are valuable in setting the baseline for understanding sediment-water interactions on a global scale.

Biscaye and Eittreim (1977) synthesized nephelometer data collected throughout the North and South Atlantic, showing areas of high concentrations in the Western North Atlantic and in the Argentine Basin. Their initial hypothesis was that the high concentrations were caused by sediment eroded and resuspended by deep boundary currents generated by cold, saline water sinking at the poles and moving equatorward. Others noted a spatial association between elevated particulate matter concentrations (PM) in nepheloid layers and eddy kinetic energy (EKE) (Hollister and McCave, 1984) or bottom trapped topographic Rossby waves (Grant et al., 1985). Nephelometer data were collected in all oceans, however, no global maps of BNL parameters were constructed from those data. More than thirty years ago the state of general understanding about nepheloid layers was reviewed by McCave (1986). Most of the transmissometer data presented and discussed in this paper were collected after that review, and the first global synthesis of the Lamont Thorndike nephelometer data is contained in this paper. The combined data sets provide a much clearer picture of global geographic distribution, intensity, and variability of the BNL. New physical oceanographic measurements and models have also improved our understanding of hydrodynamics in the ocean.

The purpose of this paper is to compare global maps of maximum bottom particle concentrations in the deep ocean, thickness of BNLs, and “excess mass” of particles integrated within BNLs compiled from the nephelometer data collected from 1964 to 1984 with the maps of the same variables compiled using transmissometer data we collected between the late 1970’s to the present (Gardner et al., 2018a). We compare these data with published distributions of EKE, benthic energy dissipation, mean near-bottom kinetic energy, and refer to newly published time-series measurements in BNLs to better understand the causes, likely location, and variability of strong and weak BNLs.

2. Methods and data

The Lamont Thorndike photographic nephelometer (Thorndike, 1975) was developed to provide quantitative turbidity profiles in the ocean. The nephelometer was mounted on a metal frame coupled with a deep-sea camera to photograph the seafloor down to >7000 m, so both instruments had to be rugged enough to withstand high pressures. . The nephelometer had a shielded source of continuous white light. The near-forward scattering signal was recorded using a photographic camera with an open shutter whose film advanced continuously at a constant rate. Due to natural light, the film was overexposed down to a depth of ~250 m, preventing measurements in water shallower than that depth and, therefore, comparisons with transmissometer data in the upper water column. Measurement depths were determined by a bourdon tube and compared with the total acoustic depth or CTD depth when available. Measurements were typically made at 100-250 m intervals through the upper, and often the entire water column. The film advance was constant; therefore, decreasing the lowering speed of the package increased the vertical resolution of measurements. In the High Energy Benthic Boundary Layer Experiment study (HEBBLE, 1978-83) measurement intervals were 15 m in the nepheloid layer with a 10 m depth accuracy (Gardner et al., 1985).

The direct light (E_D) passed through a calibrated glass attenuator and was then recorded in the middle of the 35 mm film; the outer sides of the film were exposed by light scattered forward from particles of all sizes in the water and appeared as a general fogging of the film. The film was then developed and digitized using a photo-densitometer to determine a *log* of the ratio of scattered light (E) to the direct light (E_D): $log\ E/E_D$. The optical response of each instrument was tested in the laboratory against a calibrated optical standard to ensure uniform response of each nephelometer. Data presented in this paper include only those measurements made with calibrated nephelometers, which spanned 1964 – 1984, and will be referred to as the E/E_D era. Of the >4000 profiles collected with this type of nephelometer, there were 2412 calibrated profiles from 52 expeditions used in this synthesis. See Thorndike (1975), Biscaye and Eittreim (1977), and Gardner et al. (1985) for further details.

Conversion of the nephelometer $log\ E/E_D$ values to PM concentrations was based on the Biscaye and Eittreim (1977) studies in the western North Atlantic where they filtered water samples collected simultaneously with nephelometer profiles. The regression between PM and $log\ E/E_D$ was linear up to a PM concentration of 300 $\mu g\ l^{-1}$ (r = 0.87), which was the maximum for nearly all of the E/E_D measurements outside the HEBBLE area.

Transmissometers were integrated with CTDs and lowered to the seafloor on 64 cruises occupying 6,392 stations between 1979 and 2016, and this time span will be referred to here as the c_p era. Transmissometers we used in the World Ocean Circulation Experiment (WOCE), Joint Global Ocean Flux Study (JGOFS), South Atlantic Ventilation Experiment (SAVE) and other open ocean projects up until about year 2000 were 25 cm path-length, SeaTech instruments with a 660 nm LED light source. Two cruises in the Western North Atlantic used a 1-m folded path-length SeaTech transmissometer (*Knorr* cruise 74, 1979 - HEBBLE program; and *Oceanus* cruise 134, 1983).

Data reduction methods for SeaTech transmissometers are given in Gardner et al., 1985, 1993, 2018a; Ohnemus et al., 2017) and on the Ocean Data View (ODV) web site:

(https://odv.awi.de/fileadmin/user_upload/odv/data/Transmissometer/info). A brief summary is that a transmissometer records in volts (0-5 volts (V)) the transmission (T) of light across a path of known length (r, m) and is converted to beam attenuation of light (c, m^{-1}) by the equation:

$$V/5 = T = e^{-cr}.$$

Data from transmissometers with different path lengths can be compared using this equation.

WetLabs C-STAR instruments were used on the CLIVAR Repeat Hydrography/GO-SHIP cruises after ~ year 2000. We did not have the opportunity to simultaneously collect and filter water calibration samples on CLIVAR/GO-SHIP cruises for comparison with beam attenuation. Without in situ samples we could not confirm a known concentration for the minimum values in the water column nor was there particle-free water available on the ship for calibration. Thus we resorted to using the common method proposed by SeaTech of using the cruise-average minimum of c_p on each cast. We later set this value to zero. This prevents an accurate comparison of particle minima between oceans, however, the uncertainty in measurements at the low minimum values from many different instruments deployed by many different operators over 4 decades proved this was the best solution.

We converted beam c_p to PM ($\mu g\ l^{-1}$) using the concurrent PM data from the HEBBLE program south of Nova Scotia in the western North Atlantic because it provided a large number of measurements collected synchronously over the widest range of concentrations in any deep-sea study (Gardner et al., 1985), and filtration sampling focused on the deep water, which is the subject of this synthesis. Boss et al. (2015) noted that the mass contribution of particles > 20 µm is underestimated by transmissometers due to optical responses, confirming previous observations by Gardner et al., (1993) that in-situ c_p measurements were unchanged after the fast-settling particles sank to the bottom of a water bottle. The c_p:PM correlation was very linear up to the PM concentration of 2000 $\mu g\ l^{-1}$ (r=0.97), beyond which there were insufficient data or the c_p signal was saturated for the 1-m pathlength transmissometer (%transmission = 0%). The conversion equation used was

PM ($\mu g\ l^{-1}$) = 1208 * c_p (m^{-1}).

The only expedition where a Lamont nephelometer and a transmissometer have been deployed simultaneously was during the HEBBLE cruise KN74, which included a 2.5 month deployment of a bottom tripod with both instruments collecting data simultaneously at the same location at the 1 m off the seafloor in the HEBBLE study area (Gardner et al., 1985; 2017).

Beam attenuation due to particles (c_p) is linearly correlated with particle concentration when the composition and size distribution are relatively uniform (Baker and Lavelle, 1984). However, the conversion factor to PM is neither universally constant, nor uniform throughout the water column, because particle composition and particle size distribution change seasonally in surface waters and with depth (Gardner, 1989; Gardner et al., 1993; 2001). Because we are analyzing benthic nepheloid layers, whose primary source of particles is resuspended sediment, greater uniformity can be expected in the conversion factor from c_p to PM, and from $log\ E/E_D$ to PM.

There is a small systematic difference in the response of E/E_D versus c_p between 250 m and 4000 m, due either to changes with depth in particle characteristics (size, composition) or to second-order effects of temperature or pressure on one or both of the instruments (Fig. 6 of Gardner et al., 1985). Perhaps as a result of these effects, the depth of the PM minimum in profiles differed between the two instruments in the HEBBLE program by about 900 m with the transmissometer minimums being shallower (Figs. 2, 7 of Gardner et al., 1985). There was very little change in concentration over most of the water column, so depth differences between minima may be large, but the contribution to integrated mass found in between those minima is usually relatively small. Therefore, for all assessments in this paper we are comparing PM concentrations to PM concentrations, not one optical parameter to another.

The "maximum bottom concentration" at each CTD station was determined by taking an average of the bottom 10 m of c_p data collected. For the E/E_D data we selected just the bottom value (10-15 mab) because the sampling interval was about ~30 m in the nepheloid layer for most profiles (10-15 m for HEBBLE data) compared to 2 m for beam c_p data. The distance of the instrument above bottom for each cast was not always reported, however, most cruise logs show it was generally 5-10 mab for CTD data. In the HEBBLE program the distance was narrowed to 2-7 mab using a suspended weighted bottom sensor that triggered a red light on the CTD control panel at 2 mab.

The thickness of the "full" nepheloid layer is defined as the distance between the profile minimum and the deepest measurement of E/E_D or c_p and was used to calculate the thickness and integrated excess mass in the "full" BNL. To identify the top of a "strong" BNL (defined in this paper as PM>20 µg l^{-1}), the depth of the $c_p^{minimum}$ + 0.01 m^{-1} value on each profile was used (Fig. 2). This better identifies a significant increase in PM because 0.01 m^{-1} was at the low end of resolution of the oldest transmissometers. A c_p of 0.01 m^{-1} equals about 12 $\mu g\ l^{-1}$, based on PM = 1208*c_p. Adding the typical range of minimum concentrations at the optical minima (5-12 $\mu g\ l^{-1}$) yields a range of 17-24 $\mu g\ l^{-1}$ for PM of the c_p profiles from which we calculated the thickness of the "strong" BNL and integrated excess mass in the "strong" BNL (Fig. 3a). This was in the concentration range of 20 $\mu g\ l^{-1}$ (E/E_D of 10) that we used to calculate the thickness and integrated excess mass of a "strong" BNL when processing the E/E_D data (Fig. 3b).

For the E/E_D and c_p data we mapped the integrated excess mass in the "strong" BNLs where concentrations were > 20 $\mu g\ l^{-1}$ (Fig. 3), and excess mass in the "full" BNL based on PM deeper than the particle minimum (Fig. 4). For the E/E_D data we also calculated and mapped PM concentrations at the depth of optical minima (Fig. 5).

Data for all c_p and E/E_D parameters were gridded to 1° x 1° grid, contoured, and displayed using Golden Software's Surfer package. While mapping c_p data we tested many search distances from 2° - 15° of longitude/latitude and found that using a search radius of 8° was optimal in terms of data presentation without excessive small-scale details and interpolation artifacts. Obviously, because of this, the extreme PM values were smoothed. The larger the near-bottom concentration, the more temporally variable PM concentrations are likely to be (Gardner et al., 2017). When a location is occupied more than once, the data are averaged in this process.

Lamont nephelometer measurements aren't feasible in water <250 m. Our CTD/c_p stations seldom include measurements on the shelf or upper slope; however, there are many studies that show resuspension of bottom sediments in shallow environments that will not be addressed here. Sediment has also been shown to be resuspended by breaking internal waves on tidal periods on the upper slope and in submarine canyons, creating intermediate nepheloid layers that dissipate within 20-30 km from the point of resuspension (Gardner, 1989; McPhee-Shaw et al, 2004; Puig et al., 2014 and refs therein), however, there is no direct evidence that this sediment from the upper slope contributes significantly to "strong" BNLs in most areas of the deep sea (>2000 m). (See sections of c_p in the western North Atlantic, Pacific and Indian Oceans in Supporting Material of Gardner et al., 2018 b). There are also many measurements of nepheloid layers in the Mediterranean Sea (Karageorgis et al., 2008: Puig et al., 2013a; Durrieu de Madron et al., 2017) and Gulf of Mexico (Son et al., 2009). These are not included in our data set, though we recognize the importance of those marginal seas. We have data from a few E/E_D stations in both of those regions, but not enough to characterize the BNLs in either region reasonably.

CTD/c_p data up until 2012 are available at National Centers for Environmental Information (NCEI) (http://www.nodc.noaa.gov/OC5/WOD13/) as a part on the World Ocean Database as well as from a stand-alone dataset at the Ocean Data View web site (http://odv.awi.de/en/data/ocean/). We post-processed data from 2003 to present and data are being uploaded to the CCHDO database (https://cchdo.ucsd.edu). All of the JGOFS transmissometer data we collected and processed can be found at http://usjgofs.whoi.edu/jg/dir/jgofs/. Nephelometer data are available through GeoMapApp (http://www.geomapapp.org/).

3. Results and Discussion

The data collected during these two multi-decadal time periods are not identified or sorted for seasons or years. Based on long near-bottom time-series measurements one would not expect significant seasonal impact on sediment erosion/resuspension (Gardner et al., 2017). Measurements during the E/E_D era (1964-1984) were made primarily during Lamont-Doherty Earth Observatory (LDEO) geophysical surveys with the ships stopping once or twice a day to take piston cores, bottom photos, and nephelometer profiles without temperature or salinity measurements. This sometimes resulted in stations along a straight transect, but often stations were more randomly located in an area of sub-seafloor geophysical interest rather than being driven by hydrographic hypotheses.

Conversely, the c_p era profiles were made mostly along transects during hydrographic programs seeking to determine distributions of important physical and biogeochemical variables and to develop explanatory hypotheses. Several such basin-wide transects have been occupied 2-3 times, decades apart (Gardner et al., 2018a). Most notable about these repeated transects is the similarity of particle distribution within sections except in surface waters where seasonal variability in primary production controls particle concentrations, and can increase particle concentrations at mid-water minima, but have little noticeable affect on bottom PM concentrations.

We collected the transmissometer data over a 37-year period in various seasons, and have combined the BNL data as if all were collected simultaneously. Two pieces of strong evidence justifying that approach are 1) areas of high PM concentration in the North and South Atlantic are found in the same two locations of highest concentration in Biscaye and Eittreim (1977) in the E/E_D era, regardless of season, and 2) all of the beam c_p sections that we have made from transects repeated 10-20 years apart in different oceans have shown that high and low benthic PM concentrations occur in the same areas during each transect (Gardner et al., 2018b).

It has long been recognized that benthic nepheloid layers result primarily from resuspension of bottom sediment either locally or through advection from surrounding topography. Other sources include hydrothermal vents along mid-ocean ridges (Beaulieu et al., 2013), cascading of dense shelf water (Puig et al., 2013a) and open ocean convection in areas where winter convection can reach the shelf edge (Durrieu de Madron et al. 2017; Ivanov et al., 2004; Martin et al., 2010; Puig et al., 2013b). A rare event was observed by Kao et al. (2010) in which torrential rains and erosion generated hyperpycnal flow down a canyon to >3500m. These mechanisms certainly contribute to sedimentation along continental margins and beyond, though they are not the direct primary sources of PM in strong benthic BNLs in the deep ocean basins. In this paper we map and seek to understand the processes that cause frequent resuspension events that sustain strong nepheloid layers in deep ocean basins. That is different from determining the major drivers of shelf to deep-sea transport (turbidity currents) and rates of sediment accumulation.

The fact that high and low PM concentrations during different decades consistently occur in the same regions suggests that there are regional hydrodynamic forces and/or topography that help generate currents strong enough in specific locations to erode and resuspend sediment, while in other locations currents are rarely strong enough for erosion. There is growing evidence that bottom trawling for fish is resuspending significant amounts of sediment on the shelf, upper slope and submarine canyon walls (Palanques, et al., 2006), but evidence is lacking on whether this contributes significantly to nepheloid layers in deep ocean basins unless turbidity currents are generated.

3.1. Maximum concentration near the seafloor.

The areas of maximum bottom PM concentration during the two eras (1964-1984 vs 1979-2016) match remarkably well on global scales (Fig. 1). High concentrations are found in relatively few areas of the ocean and are well correlated with areas of high eddy kinetic energy. The matching PM maxima in the western North Atlantic were detected by both instruments (E/E_D and c_p) used during the HEBBLE program where the highest global values were recorded. Concentration of filtered samples frequently exceeded 500 $\mu g\ l^{-1}$ and reached a maximum of 12,700 $\mu g\ l^{-1}$ at 2 mab, 8,500 $\mu g\ l^{-1}$ at 16 mab, and 2,100 $\mu g\ l^{-1}$ at 131 mab during one cast. Percent transmission dropped to 0% throughout the bottom 50 m of the down profile. It is conceivable that we sampled the tail end of a turbidity current. High PM concentration was also recorded in this region during other sampling times in both eras (Hayes et al., 2015b; Gardner et al., 2018b).

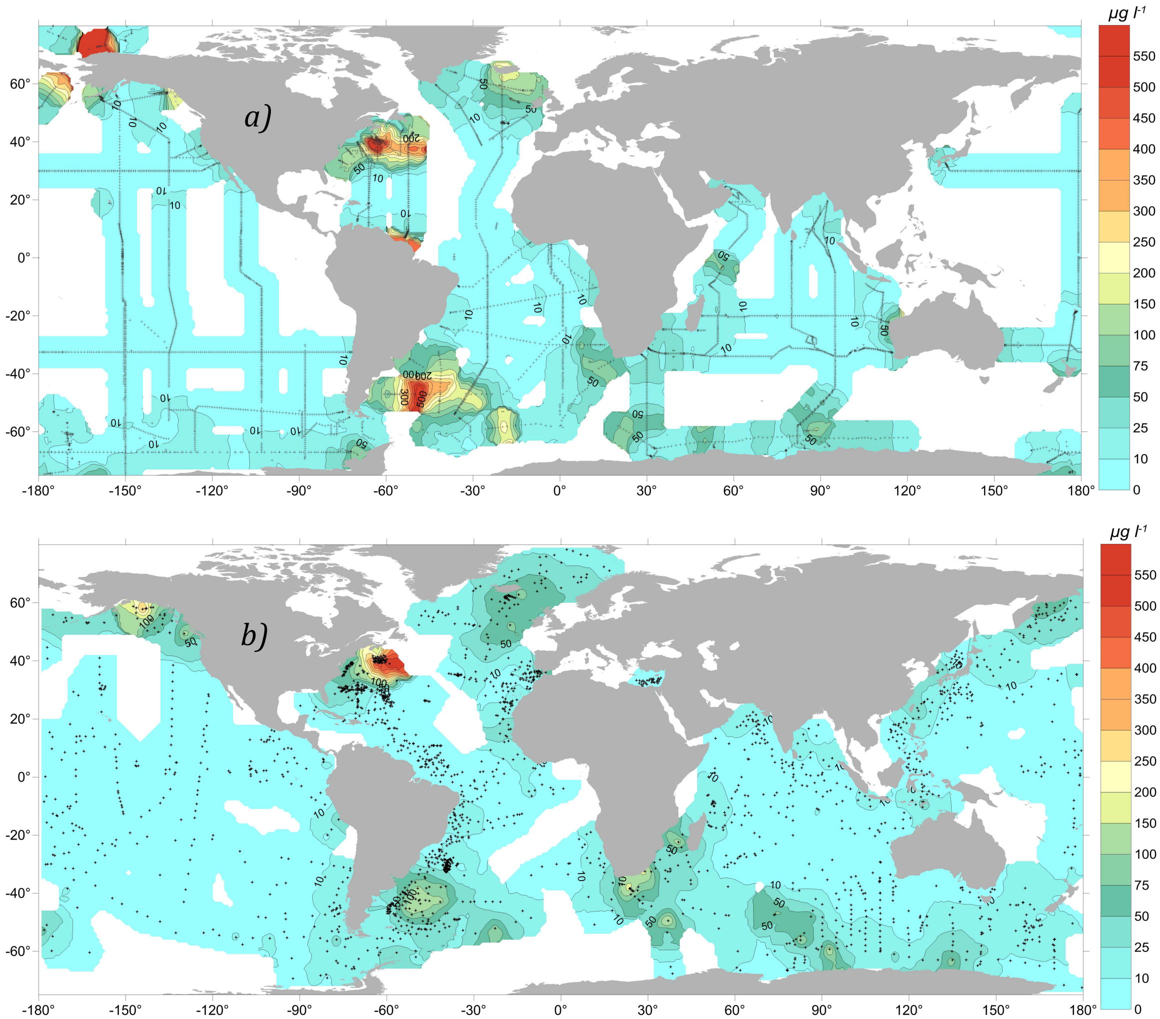

Figure 1. a) Particulate matter concentration ($\mu g\ l^{-1}$) averaged in the bottom 10 m of each c_p profile. b) Particulate matter concentration ($\mu g\ l^{-1}$) measured at the bottom depth of each E/E_D profile. Scales are not linear in order to illustrate finer detail at lower concentrations.

PM concentrations were high in the Argentine Basin during both eras, though substantially higher during the c_p era, when far more data were collected. Moored near-bottom time series measurements of c_p and currents across the Argentine Basin show that benthic storms create large temporal and spatial variability in PM concentrations near the seafloor in the center of the basin (Richardson et al., 1993), so differences between eras could result from this innate variability. PM concentrations were low and steady at moorings 1 and 2 at 2000 m and 4500 m. Elevated PM concentrations didn't appear until moorings 3-5 at 5000, 5300 and 5000 m, well away from the continental slope and the bottom western boundary current.

PM concentrations were higher in the Gulf of Alaska in the E/E_D era than in the c_p era, but elevated values were found mostly in slope water, not the deep ocean. Differences could result from both temporal variability as well as sampling in different areas. High PM concentrations were measured on either side of the Bering Strait during the c_p era, with very high concentrations on the shelf in the Arctic. Those areas were not sampled during the E/E_D era, so no comparison can be made. Conversely, elevated PM values were measured northeast of Kamchatka (NW Pacific) during the E/E_D era, but no data were collected there during the c_p era for comparison. PM was generally higher around Iceland in the c_p era than in the E/E_D era, due possibly to seasonal differences.Concentrations around South Africa were comparable in both eras, but had a more varied distribution in the c_p era. High PM concentrations occurred in seemingly random places in the Southern Ocean during both eras, which may be caused by the abundance and variability of non-linear eddies in the Southern Ocean (Chelton et al., 2011; Gardner et al., 2018a, Fig. A4; Gardner et al., 2018b, Figs. S4-S5). The region northwest of the Amazon outflow showed elevated PM concentrations in the c_p era, but not in the E/E_D era. The high PM values detected were in the shallow water c_p profiles (<400 m) in two occupations of those transects and appear to be related to outflow from the Amazon and Orinoco Rivers, which clearly vary seasonally.

Most of the seafloor away from continental margins and the "hot" spots described above has very low PM concentrations ($<10\ \mu g\ l^{-1}$), indicating little or no resuspension of sediment. Of course, there must be erodible sediment to create BNLs. It is noteworthy that only a few mm of sediment are required to create the BNLs in the deep ocean.

The E/E_D profiles were made primarily in deep water. Less than 2% of stations were shallower than 1000 m and only 9% were shallower than 2000 m. The E/E_D data were usually measured at ~250 m intervals through the upper water column below 250 m and every 30-100 m in the bottom 1000 m and at the deepest depth. As a result, E/E_D profiles are less likely to reveal any intermediate layers emanating from continental margins. The hydrographic transects during the c_p era occasionally had a few stations across the continental slope, but intermediate nepheloid layers are not obvious in most of our transects across continental margins. Intermediate layers have been recorded in margin studies elsewhere (e.g. McCave and Dickson, 1986; McPhee-Shaw et al., 2004). Stations in both eras were seldom close to mid-ocean ridge axes, where hundreds of hydrothermal vents have been identified by increased temperature, turbidity, iron or other elements (Beaulieu et al., 2013; Fitzsimmons et al., 2017). Temperature or salinity measurements were rarely made at E/E_D stations.

3.2. "Strong" Nepheloid Layer Thickness, PM>20 $\mu g\ l^{-1}$

The map of "strong" nepheloid layers (PM >20 $\mu g\ l^{-1}$, see section 2. Methods) generally shows thick BNLs where near-bottom PM concentrations were elevated during the c_p era (Fig. 2a). Notable concentration/thickness anomalies occur southwest and southeast of the horn of Africa beneath the Agulhas retroflection. Other concentration/thickness anomalies exist around Madagascar and west of Australia (compare Figs. 1 and 2). Anomalies in magnitude between maximum PM and layer thickness during the E/E_D era are observed south of Alaska, west of Chile, and west of Europe (Fig. 2b). Those areas are all along continental margins. The stations around Alaska and west of Europe tend to be shallower than 2000 m.

3.3. Integration of excess mass in "strong" nepheloid layers.

The excess PM mass ($\mu g\ cm^{-2}$) in BNLs that we define as "strong" (PM>20 $\mu g\ l^{-1}$) yields a more robust quantification of erosion and resuspension of bottom sediments than just the maximum near-bottom concentration or thickness of the BNL (Fig. 3a, b). The regions of thick, "strong" BNLs overlap well with the regions of highest integrated excess PM during both eras, as would be expected (Fig. 3). Greater variability exists in the Southern Ocean between the two eras. This is not surprising as the Circumpolar Current and the non-linear eddies it generates are less constrained by continental margins and thus occur more randomly, similar to the randomness of Gulf Stream rings. The areas in the Western North Atlantic where bottom concentrations exceeded 500 $\mu g\ l^{-1}$ during both eras (Fig. 1) matches well, and were recorded by both instruments used simultaneously in the HEBBLE program where benthic storms were active beneath the Gulf Stream meanders/rings (Gardner et al., 2017). In the Argentine Basin bottom concentrations and intense BNL thicknesses are smaller during the E/E_D era, though still significant.

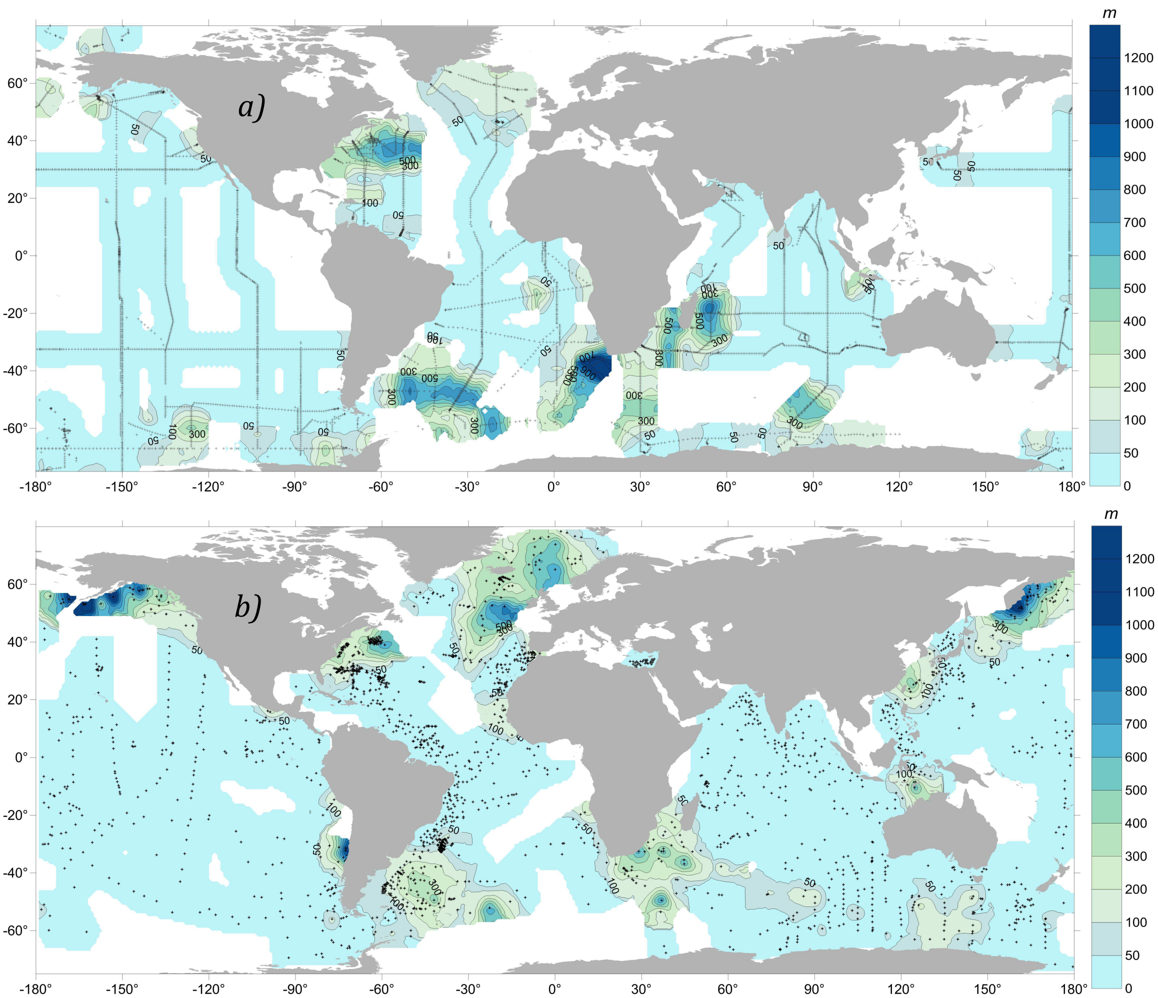

Figure 2. Thickness of the “strong” (>20 $\mu g\ l^{-1}$) nepheloid layer (m) based on a) c_p profiles, and b) E/E_D profiles. Note scale change at 100 m thickness.

In maps of both integrated excess mass and nepheloid layer thickness (Figs. 2, 3), the area southwest of Africa beneath the Agulhas retroflection is more prominent than bottom PM concentrations during the c_p era. Similarly, nepheloid layer thickness in areas south and east of Madagascar are greater than in most regions of the ocean suggesting that resuspended sediment was advected laterally from the lower continental slope and upper rise. These regions are known to have strong meanders in currents that break off and form rings like those in the Gulf Stream (Penven et al., 2006). Sampling in this area was much less frequent during the E/E_D era. Bottom photographs in this area also provide abundant evidence of currents strong enough to erode and move seafloor sediment (Hollister and Nowell, 1991).

The thick BNLs with only modest excess PM south and east of Iceland during the E/E_D era are often in relatively shallow water (<2000-3000 m) or are on the slope leading to deeper water (Figs. 2b, 3b). These areas may be affected by lateral, down-slope transport from the shallow Rockall or Porcupine Banks (Fig. 2b) (McCave and Dickson, 1986). Nepheloid layers appear to the west of North Africa during the E/E_D era, but sampling did not occur close to the African continent during the c_p era. Similar paucity of sampling possibly explains temporal differences in the existence of thick or high PM nepheloid layers around Alaska, Kamchatka, and Australia.

Earlier we justified our comparison of PM concentrations during the E/E_D and c_p eras in order to extend the period of time sampled during the two eras to 52 years and augment the data coverage. It is therefore useful to combine all data into a single map of “strong” BNLs (Fig. 3c). This figure accentuates the point that much of the ocean is devoid of “strong” BNLs except near land or at a few hot spots beneath areas of high EKE.

3.4. Excess mass in “full” BNLs from profile minimum to bottom value.

Integrating the excess mass of PM below the c_p or E/E_D minimum for both eras (Fig. 4) shows more spatial variability than in maps of just the strong BNL (Fig. 3). Few areas have more excess PM than 1000 µg cm^{-2} (Fig 4). The cp data show more areas with moderate BNLs. Two influences are that the cp minima are generally 900 m shallower than the E/ED minima, yielding higher excess mass, and the cp data have a much smaller sampling interval (2 m), which means that below the minimum there is a greater likelihood for higher values for integration. The “full” BNL using E/ED is comparable to the integration of Biscaye and Eittreim (1977).

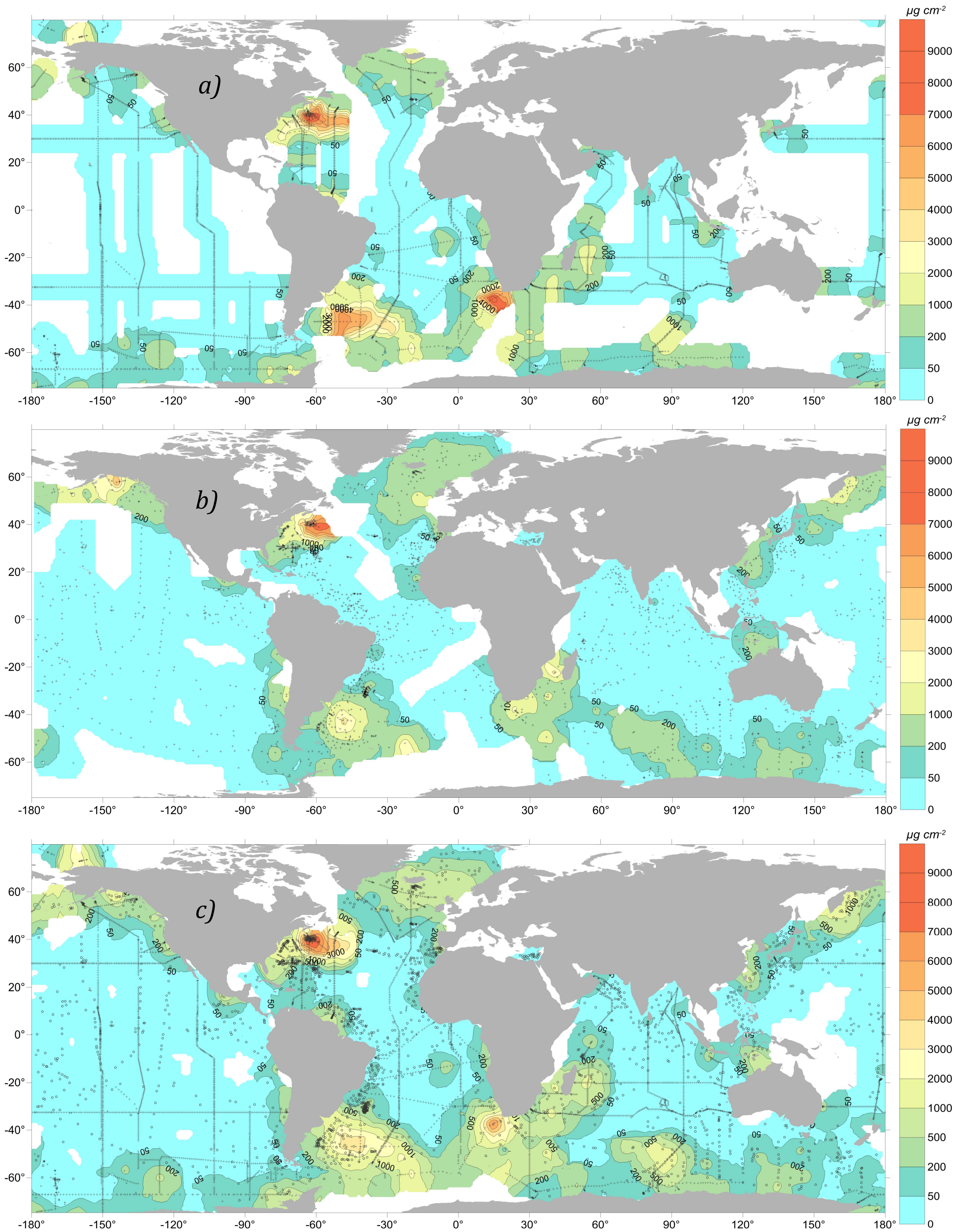

Figure 3. Excess particulate matter in “strong” nepheloid layers (>20 $\mu g\ l^{-1}$) based on: a) c_p profiles, b) E/E_D profiles, and c) combined data from a) and b). Note scale changes between 0 and 1000 $\mu g\ cm^{-2}$. See section 2 for calculation.

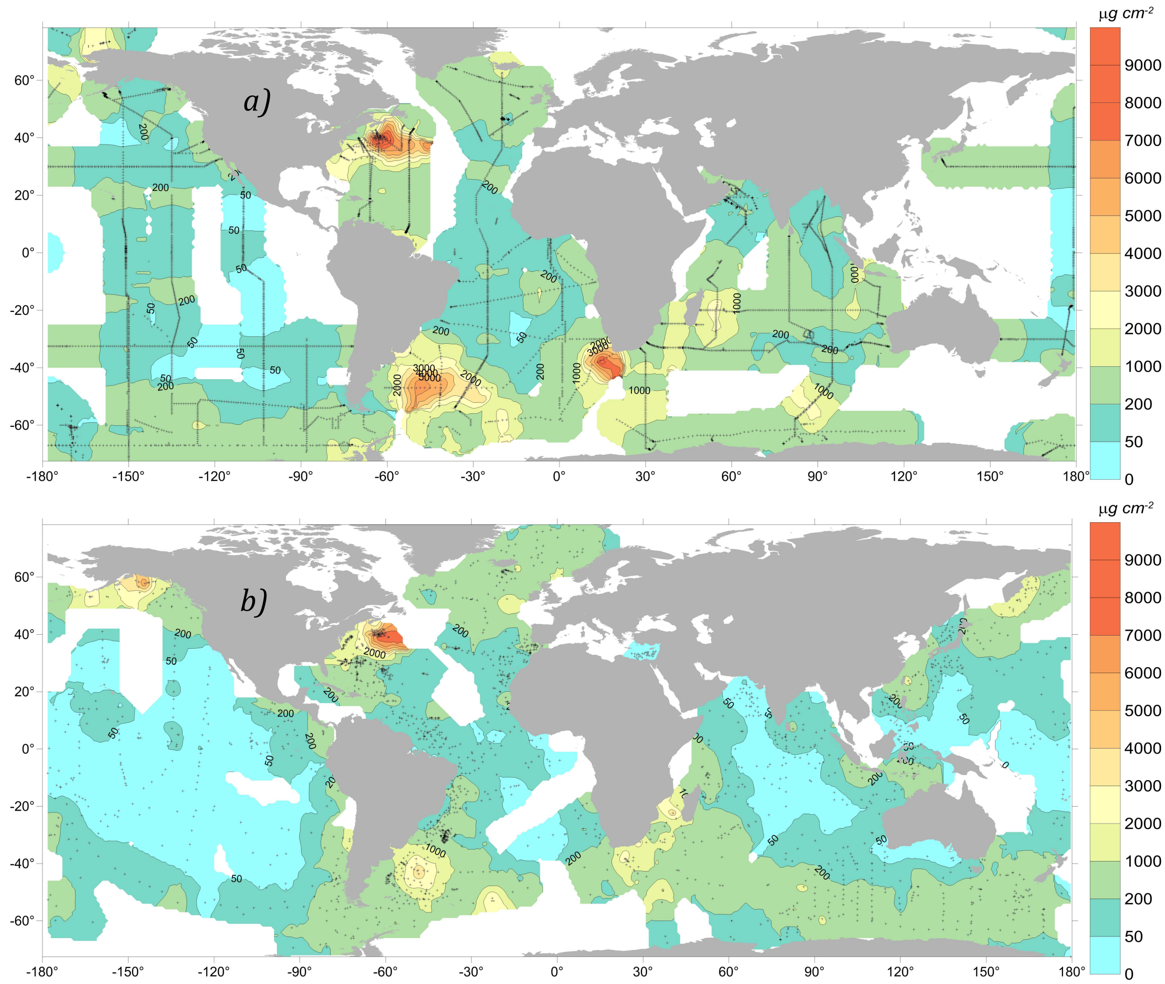

Figure 4. a) Excess Particulate Matter ($\mu g\ cm^{-2}$) below the c_p minimum. b) Excess Particulate Matter ($\mu g\ cm^{-2}$) below nephel minimum based on E/E_D data. Note scale change below 1000 $\mu g\ cm^{-2}$ to illustrate finer detail. See section 2 for calculation.

There are large expanses of the oceans, especially the Pacific, that have little to no BNL. In vertical sections of c_p data (Gardner et al., 2018b), the small increases in those BNLs of low PM seem limited to the elevation of the surrounding topography, suggesting that resuspension in these areas is more a process of slight velocity increases causing minor erosion around bottom hills and lateral advection of resuspended sediment, or perhaps generation of enough boundary layer turbulence to inhibit particle deposition at depths below the surrounding topographic features.

3.5. PM concentration at E/E_D minimum.

PM concentrations at the E/E_D minimum are low globally: <21 $\mu g\ l^{-1}$. Biscaye and Eittreim (1977) showed that the lowest PM concentrations at the minimum in the E/E_D profiles are located in the center of the oceanic gyres in the North and South Atlantic. Additional E/E_D data collected in the Atlantic since then maintain the same general distribution (Fig. 5). The central gyres of the North and South Pacific and the Indian Ocean also have similarly low PM concentrations at the profile minimums. PM concentrations are slightly higher along the equatorial upwelling regions in all three oceans, as would be expected beneath areas of elevated surface primary production. The highest PM concentrations at the E/E_D minimum tend to be in shallower regions around Alaska and Iceland or along continental margins, which is where higher surface production could also occur. Continental margins obviously also provide a potential source of sediment for lateral transport throughout the water column. Note the increase of PM west of North Africa where winds are known to cause upwelling and carry Saharan dust to the ocean (Prospero and Carlson, 1981), enhancing primary production. East of Argentina, Patagonian dust enhances primary production in the South Atlantic (Johnson et al., 2011). The E/E_D minima are also high beneath the productive upwelling regions west of South Africa, Namibia, and Peru.

3.6. Seasonal bias in nepheloid layers?

Might seasonal variations in the PM concentration in nepheloid layers create a bias in the data? Evidence from in situ time-series photographs (Lampitt, 1985) and sediment trap fluxes (Deuser, 1980; Honjo et al., 2008) demonstrate that many areas of the ocean experience seasonal variations in the downward flux of organic detritus from surface waters, however, we know of no evidence of seasonality in near-bottom PM concentrations other than seasonal cascading of water in the Mediterranean (e.g. Canals et al. 2006; Puig et al., 2013a; Durrieu de Madron et al., 2017), and at many margins around the world, with most cascading sinking to <250 m (Ivanov et al., 2004). The Gulf Stream exhibits some seasonal changes in sea surface height (Kelly, 1991), but we know of no evidence of seasonal variations in ring formation, meander behavior, or bottom currents sufficient to resuspend sediments and create areas of intense nepheloid layers. Episodic benthic storms have been documented in the Western North Atlantic (Gardner and Sullivan, 1981; Hollister and McCave, 1984; Isley et al. 1990; Gardner et al., 2017), however, there is no evidence of seasonality in their occurrence.

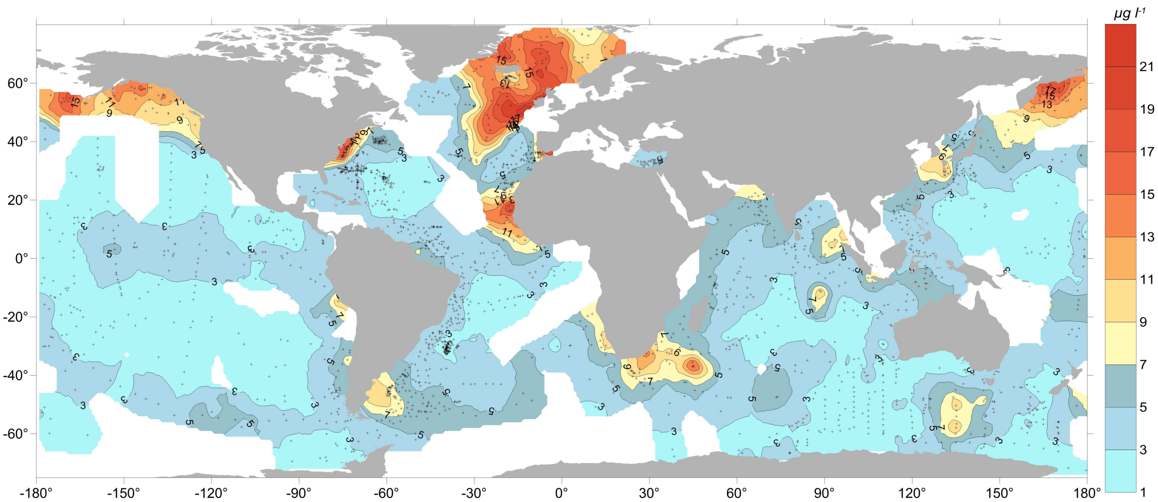

Figure 5. Particulate matter concentration ($\mu g\ l^{-1}$) at the depth of E/E_D minimum in the water column based on E/E_D data.

3.7. Causes of “strong” nepheloid layers

Hollister and McCave (1984) noted a general global correlation among spreading of cold bottom water, “strong” BNLs and high surface eddy kinetic energy generated by features such as the Gulf Stream and its warm- and cold-core rings, suggesting that sediment resuspended could be diffused or mixed upward, or advected laterally. Hydrographic bottom boundary layer thickness is usually less than 100 m, depending on bottom topography, slope, and current speeds (Armi and Millard, 1976), yet nepheloid layers can be > 1000 m (Fig. 2). Armi (1978) argued that thick BNLs were caused by sediment being advected laterally because deep ocean eddy diffusivity is too small to explain diffusional mixing for clay particles up to 1000 m. Watts et al. (1995) and Andres et al. (2016) have shown that beneath the meanders of the Gulf Stream, deep underwater cyclones and anticyclones are generated that create currents strong enough to resuspend sediment in waters much deeper than the Deep Western Boundary Current (DWBC), which extends only to ~4000 m depth in the Western North Atlantic. Water deeper than

4000 m in this area consists mainly of Antarctic Bottom Water (AABW) based on high silicate concentrations (Richardson et al., 1981).

Using an eddy-resolving ocean model, Thran et al., (2018) found that contourite sediment drifts in all oceans were most likely to develop in areas with frequent high-energy bottom current fluctuations that could erode, transport and deposit sediment in specific areas. They also acknowledged the potential role of upper ocean dynamics in controlling drift accumulation through direct influence from deep eddy circulation.

Gardner et al., (2017) compared the surface EKE with PM concentrations and temporal variability in benthic PM concentration and found a tight correlation. They concluded that the DWBC speeds were too weak by themselves to generate intense nepheloid layers. Benthic storms with current speeds >~20 $cm\ s^{-1}$, caused by cyclogenesis or bottom-trapped topographic Rossby waves, were required to erode the seafloor. Periods of lower concentrations were times of PM deposition. PM concentrations between storms were still elevated compared with the weak to non-existent BNLs in areas of low EKE that encompass much of the world’s ocean. Lateral mixing away from boundaries is still required to develop nepheloid layers hundreds of meters thick. This could occur along continental margins or as water moves past abyssal hills and seamounts in the ocean that Turnewitsch et al., (2013) point out are more abundant than is generally recognized.

The high values of bottom current intensities and variability in the maps produced from the ocean model of Thran et al., (2018) match well overall with areas of high global surface EKE that was visualized by Dixon et al., (2011) or Wunsch (2015). The maps reveal marked similarities between surface EKE and BNL intensity (Figs. 2, 3, 6). In addition to the Western North Atlantic, good correlation between EKE and BNL intensity is found in the Argentine Basin as previously noted by Hollister and McCave (1984) and Richardson et al. (1993). Time series transmissometer and current measurements near the seafloor provided evidence of benthic storms in the Argentine basin that are correlated with high surface EKE caused by confluences, meanders, and eddies spun off from the Brazil (southward flowing) and Malvinas (northward flowing) boundary currents

(Richardson et al., 1993). Flow through the Mozambique Channel between Madagascar and Africa usually occurs as eddies rather than a steady current (Penven et al., 2006). The Agulhas Current spawns rings at the Agulhas retroflection south of Africa. This eddying motion correlates well with relatively "strong" BNLs from Madagascar around the Horn of Africa to southwest of Africa where concentrations are most intense where the current reverses course and moves to the southeast (Figs. 2, 3).

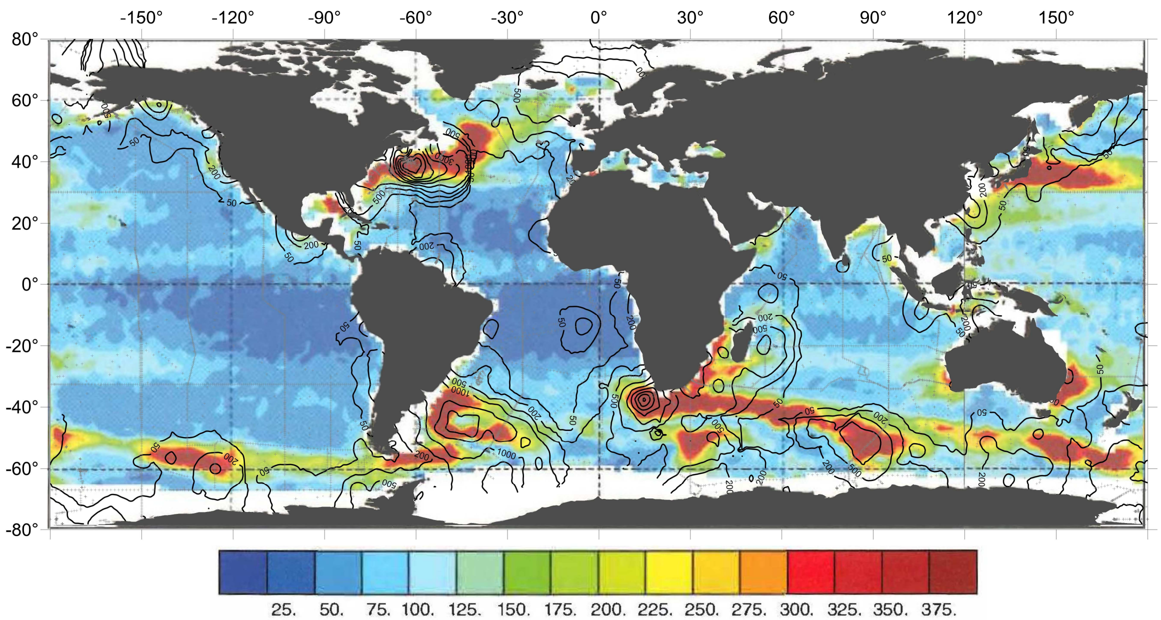

Figure 6. An estimate of the temporal variability about the mean of kinetic energy per unit mass, cm^2s^{-2}, in the ocean, derived from four years of altimetric data and using the geostrophic relationship (adapted from Wunsch, 2015, and personal communication, Wunsch, 2018) with contours of Excess Particulate Matter in "strong" nepheloid layers (>20 $\mu g\ l^{-1}$ from Fig. 3c) superimposed. Stations shown in grey.

3.8. Are there nepheloid layers beneath the Kuroshio?

Gardner et al., (2018a) noted that the greatest anomaly when comparing surface EKE and benthic nepheloid layers based on existing data is the area beneath the Kuroshio Extension off of Japan. Like the Gulf Stream, the Kuroshio Extension is a strong surface western-boundary current that meanders and sheds eddies in a manner similar to the Gulf Stream. They noted some differences in bottom topography (trench versus nearby continental slope) and lack of bottom water formation creating a deep western boundary current in the Pacific, but lacked the c_p data to provide a decisive answer regarding bottom concentrations or variability. In the present paper (Figs. 1b, 2b, 3b) there are a few E/E_D profiles beneath the Kuroshio Extension, but none show significant nepheloid layers. More measurements are needed there to elucidate the differences.

3.9. Other correlations between nepheloid layers and seafloor dynamics

In addition to comparing surface EKE with BNL intensities, we have compared c_p nepheloid layer distributions with detailed global maps of mean kinetic energy at 50 mab (Fig. 2 of Arbic et al., 2010) as well as equally detailed global maps of energy dissipation in the bottom boundary layer (Figs. 5 and 9 of Arbic et al., 2009; Fig. 3 of Wright et al., 2013). There is significant agreement between their maps of energy dissipation and the maps of surface EKE in the vicinity of the Gulf Stream, the Agulhas current, in the Argentine Basin, and in spots beneath the Antarctic Circumpolar Current (ACC). Given that the areas of higher EKE in the circumpolar current are likely due to eddies (Chelton et al., 2007), their geographic location may be less constrained than in the areas of high EKE unless they encounter topographic constraints like the Drake Passage or features like the Kerguelen Islands where eddies might be generated more frequently.

Observations also show high energy dissipation rates due to bottom boundary drag beneath the Kuroshio between 32°-38°N. Conversely, maps of modeled mean kinetic energy at 50 mab show similarly maximal values in all of the regions of high EKE except beneath the Kuroshio, where mean kinetic energy is about half of that beneath the Gulf Stream and Argentine Basin currents (Fig. 2 of Arbic et al., 2010).

A map of modeled mean annual bottom kinetic energy (Thran et al., 2018) shows high values in the western North Atlantic, Argentine Basin, South of Africa, and several locations beneath the ACC. Beneath the Kuroshio, EKE is higher than the surrounding seafloor, but much lower than the afore mentioned areas of expected and measured high EKE. Our data sets do not show strong BNLs in the Kuroshio extension region.

3.10. Geochemical relevance

Radionuclides such as ^{230}Th and ^{231}Pa are used as paleo- and modern proxies for estimating vertical PM fluxes to the seafloor and lateral fluxes of insoluble elements to and from continental margins as well as understanding the southward flux of North Atlantic deep water and other aspects of ocean circulation. Studies in the Geochemical Tracers program (GEOTRACES) have found that PM scavenges these adsorption-prone radionuclides that are also used as quantitative tracers of adsorption to sinking particles in the ocean (Hayes et al., 2015a,b; Van Hulten et al., 2017). Combining the E/E_D data with the more recent c_p data improves our confidence that particle scavenging is persistent in known locations over long periods of time, yet large areas of the ocean experience little to no erosion or resuspension of sediment to enhance scavenging. With this knowledge, adjustments can then be made to better interpret radionuclide deposition throughout the ocean. An improved understanding of which driving forces are important (EKE, topographic waves, cyclones and anticyclones spun up beneath meanders and rings of strong boundary currents) and where PM in the benthic nepheloid layer is sourced, transported, and deposited will help to determine oceanic locations where such scavenging is most likely to occur and to assess its impact on present and past global biogeochemical questions.

4. Conclusions

The regions of “strong” benthic nepheloid layers are very similar during both the 1964 to 1984 period as well as from the 1980’s to present day. “Strong” BNLs and benthic storms are most intense and thickest beneath areas of high surface and bottom eddy kinetic energy, strongly suggesting a linkage with upper ocean dynamics. This connection is best explained by generation of cyclones/anticyclones beneath meanders/rings spun off by major surface boundary currents or from bottom-trapped topographic waves that episodically create and maintain “strong” BNLs. The geographic locations of intense and thick BNLs also coincide with areas of high-energy dissipation in the bottom boundary layer and with mean kinetic energy at 50 mab. One anomaly from this connection may be the Kuroshio Extension where data on bottom currents exist, but only a few PM data from 1964-1984 are known. Energy dissipation is high beneath the Kuroshio, however, mean kinetic energy at 50 mab is lower there than in other areas of high benthic PM. Near-bottom PM profiles and time-series data are needed to better understand this apparent anomaly.

The areas of weak to no BNLs cover similar large areas during both sampling periods. These areas include large portions of the Pacific, Atlantic and Indian oceans and are generally areas of low eddy kinetic energy.

PM scavenges adsorption-prone radionuclides that are used as paleo-productivity proxies and for investigation and modeling of modern and paleo-ocean circulation. The addition of nephelometer data from previous decades increases our confidence that areas of “strong” and weak nepheloid layers are quite consistent over time and will help to determine where resuspension scavenging is most likely to occur and to assess its potential impact on global biogeochemistry of sediments and bottom water.

References

Andres, M., Toole, J.M., Torres, D.J., Smethie Jr., W.M., Joyce, T.M., Curry, R.G., 2016. Stirring by deep cyclones and the evolution of Denmark Strait overflow water observed at line W. *Deep-Sea Research Part I*, 109, 10-26.

Arbic, B.K., Shriver, J.F., Hogan, P.J., Hurlburt, H.E., McClean, J.L., Metzger, E.J., Scott, R.B., Sen, A., Smedstad, O.M., Wallcraft, A.J., 2009. Estimates of bottom flows and bottom boundary layer dissipation of the oceanic general circulation from global high-resolution models. *Journal of Geophysical Research* 114, C02024, doi:10.1029/2008JC005072.

Arbic, B.K., Wallcraft, A.J., Metzger, E.J., 2010. Concurrent simulation of the eddying general circulation and tides in a global ocean model. *Ocean Modeling* 32, 175 - 187.

Armi, L., 1978. Mixing in the deep ocean - the importance of boundaries. *Oceanus* 21, 14-19.

Armi, L., Millard Jr, R.C., 1976. The bottom boundary layer of the deep ocean. *Journal of Geophysical Research* 81, 4983–4990, doi:10.1029/JC081i027p04983.

Baker, E.T., Lavelle, J.W., 1984. The effect of particle size on the light attenuation coefficient of natural suspensions. *Journal of Geophysical Research* 89: 8197-8203.

Beaulieu, S.E., Baker, E.T., German, C.R., Maffei, A., 2013. An authoritative global database for active submarine hydrothermal vent fields, *Geochem. Geophys. Geosys.*, 14, 4892–4905, doi:10.1002/2013GC004998.

Bartz, R., Zaneveld, J.R.V., Pak, H., 1978. A transmissometer for profiling and moored observations in water, SPIE, 160 *Ocean Optics V*, 102-108.

Biscaye, P.E., Eittreim, S.L., 1974. Variations in benthic boundary layer phenomena; nepheloid layers in the North American Basin. In: R. Gibbs (Editor), Suspended Solids in Water. Plenum, New York, N.Y., pp.227--260.

Biscaye, P.E., Eittreim, S.L., 1977. Suspended particulate loads and transports in the nepheloid layer of the abyssal Atlantic Ocean. *Marine Geology* 23, 155-172.

Boss, E., Guidi, L., Richardson, M.J., Stemmann, L., Gardner, W., Bishop, J.K.B., Anderson, R.F., Sherrell, R.M., 2015. Optical techniques for remote and in-situ characterization of particles pertinent to GEOTRACES, *Progress in Oceanography*, doi: http://dx.doi.org/10.1016/j.pocean.2014.09.007

Brewer, P.G., Spencer, D.W., Biscaye, P.E., Hanley, A., Sachs, P.S., Smith, C.L., Kadar, S., Fredericks, J., 1976. The distribution of particulate matter in the Atlantic Ocean. *Earth and Planetary Science Letters* 32, 393-402.

Canals, M., Puig, P., de Madron, X. D., Heussner, S., Palanques, A., Fabres, J., 2006. Flushing submarine canyons, *Nature*, 444, 354–357, doi:10.1038/nature05271.

Chelton, D. B., Schlax, M.G., Samelson, R.M., 2011. Global observations of non-linear mesoscale eddies, *Progress in Oceanography* 91, 167-216. doi:10.1016/j.pocean.2011.01.002.

Deuser, W. G., Ross, E. H., 1980. Seasonal change in the flux of organic carbon to the deep Sargasso Sea, *Nature* 283, 364-365.

Dixon, K.W. Delworth, T.L., Rosati, A.J., Anderson, W., Adcroft, A., Balaji, V., Benson, R., Griffies, S.M., Lee, H-C., Pacanowski, R.C., Vecchi, G.A., Wittenberg, A.T., Zeng, F., Zhang, R., 2011. Ocean circulation features of the GFDL CM2.6 & CM2.5 high-resolution global coupled climate models. WCRP Open Science Conference, October 2011, Denver, Colorado.

Durrieu de Madron, X., Ramondenc, S., Berline, L., Houpert, L., Bosse, A., Martini, S., 2017. Deep sediment resuspension and thick nepheloid layer generation by open-ocean convection. *Journal of Geophysical Research: Oceans*, 122, 2291–2318. DOI: 10.1002/2016JC012062Fitzsimmons, J.N., John, S.G., Marsay, C.M., Hoffman, C.L., Nicholas, S.L., Toner, B.M., German, C.R., Sherrell, R.M., 2017. Iron persistence in a distal hydrothermal plume supported by dissolved-particulate exchange. *Nature Geoscience* 10, 195-201, doi:10.1038/ngeo2900.

Gardner, W. D., 1989. Periodic resuspension in Baltimore Canyon by focusing of internal waves. *Journal of Geophysical Research* 94:18185-18194.

Gardner, W.D., Biscaye, P.E., Zaneveld, J.R.V., Richardson, M.J., 1985. Calibration and comparison of the LDGO nephelometer and the OSU transmissometer on the Nova Scotian Rise. *Marine Geology* 66, 323-344, 1985a.

Gardner, W. D., Blakey, J. C., Walsh, I.D., Richardson, M.J., Pegau, S., Zaneveld, J.R.V., Roesler, C., Gregg, M.C., MacKinnon, J. A., Sosik, H.M., Williams, A. J., III, 2001. Optics, particles, stratification and storms on the New England continental shelf. *Journal of Geophysical Research* 106: 9473-9497.

Gardner, W.D., Sullivan, L.G., 1981. Benthic storms: Temporal variability in a deep ocean nepheloid layer. *Science* 213, 329-331.

Gardner, W.D., Tucholke, B.E., Richardson, M.J., Biscaye. P.E., 2017. Benthic storms, nepheloid layers, and linkage with upper ocean dynamics in the Western North Atlantic. *Marine Geology* 385, 304-327, http://dx.doi.org/10.1016/j.margeo.2016.12.012.

Gardner, W.D., Mishonov, A.V., Richardson, M.J., 2018a. Decadal Comparisons of Particulate Matter in Repeat Transects in the Atlantic, Pacific, and Indian Ocean Basins. *Geophysical Research Letters* 45, 277-286. https://doi.org/10.1002/2017GL076571.

Gardner, W.D., Richardson, M.J., Mishonov, A.V., 2018b. Global Assessment of Benthic Nepheloid Layers and Linkage with Upper Ocean Dynamics. *Earth and Planetary Science Letters* 482, 126–134. https://doi.org/10.1016/j.epsl.2017.11.008.

Gardner, W. D., Walsh, I.D., Richardson, M J., 1993. Biophysical forcing of particle production and distribution during a spring bloom in the North Atlantic. *Deep-Sea Research* 40, 171-195.

Grant, W.D., Williams III, A.J., Gross, T.F.A., 1985. Description of the bottom boundary layer at the HEBBLE site: Low frequency forcing, bottom stress and temperature structure. *Marine Geology* 66, 219-241.

Hayes, C.T., Anderson, R.F., Fleisher, M.Q., Huang, K.-F., Robinson, L.F., Lu, Y., Cheng, H., Edwards, R.L. Moran, S.B., 2015a. ^{230}Th and ^{231}Pa on GEOTRACES GA03, the U.S. GEOTRACES North Atlantic transect, and implications for modern and paleoceanographic chemical fluxes. *Deep Sea Research Part II*: Topical Studies in Oceanography 116, 29-41, doi:http://dx.doi.org/10.1016/j.dsr2.2014.07.007.

Hayes, C.T., Anderson, R.F., Fleisher, M.Q., Vivancos, S.M., Lam, P.J., Ohnemus, D.C., Huang, K-F., Robinson, L.R., Lu, Y., Cheng, H., Edwards, L., Moran, S.B., 2015b. Intensity of Th and Pa scavenging partitioned by particle chemistry in the North Atlantic Ocean. *Marine Chemistry*, 170, 49-60, doi: 10.1016/j.marchem.2015.01.006.

Hill, P.S., Boss, J E., Newgard, P., Law, B.A., Milligan, T.G., 2011. Observations of the sensitivity of beam attenuation to particle size in a coastal bottom boundary layer, *Journal of Geophysical Research* 116, C02023, doi:10.1029/2010JC006539.

Hollister, C.D., McCave, I.N., 1984. Sedimentation under deep-sea storms. *Nature* 309. 220-222.

Honjo, S., Manganini, S.J., Krichfield, R.A.,, Francois, R., 2008. Particulate organic carbon fluxes to the ocean interior and factors controlling the biological pump: A synthesis of global sediment trap programs since 1983. *Progress in Oceanography* 76(3): 217-285. doi: 10.1016/j.pocean.2007.11.003.

Isley, A.E., Pillsbury, R.D., Laine, E.P., 1990. The genesis and character of benthic turbid events, northern Hatteras Abyssal Plain. *Deep-Sea Research* 37, 1099-1119.

Ivanov, V.V., G.I. Shapiro, J.M. Huthnance, D.L. Aleynik, P.N. Golovin, 2004. Cascades of dense water around the world ocean. *Progress in Oceanography*, 60: 47-98.

Jerlov, N.C., 1953, Particle distribution in the ocean. *Reports of the Swedish Deep-Sea Expedition* 3, 73-97.

Johnson, K.S., Berelson, W.M., Boss, E.S., Chase, Z., Claustre, H., Emerson, S.R., Gruber, N., Körtzinger, A., Perry, M.J., Riser, S.C., 2009. Observing biogeochemical cycles at global scales with profiling floats and gliders: prospects for a global array. *Oceanography* 22, 216-225.

Johnson, M. S., Meskhidze, N., Kiliyanpilakkil1, V.P., Gasso, S., 2011. Understanding the transport of Patagonian dust and its influence on marine biological activity in the South Atlantic Ocean. *Atmospheric Chemistry and Physics*, 11, 2487–2502.

Karageorgis, A., Gardner, W.D., Georgopoulos, D., Mishonov, A.V., Krasakopoulou, E., Anagnostou, C., 2008. Particle dynamics in the Eastern Mediterranean Sea: a synthesis based on light transmission. PMC and POC archives (1991-2001), *Deep-Sea Research I* 55: 177-202. DOI: 10.1016/j.dsr.2007.11.002.

Kao, S.J., Dai, M., Selvaraj, K., Zhai, W., Cai, P., Chen, S.N., Yang, J.Y.T., Liu, J.T., Liu, C.C., Syvitski, J.P.M., 2010. Cyclone-driven deep sea injection of freshwater and heat by hyperpycnal flow in the subtropics. *Geophysical Research Letters* L21702, doi:10.1029/2010GL044893.

Kelly, K.A., 1991. The meandering Gulf Stream as seen by the Geosat altimeter: surface transport, position and velocity variance from 73° to 46°W. Journal of Geophysical Research, 96, 16721-16738.

Lampitt, R.S., 1985. Evidence for the seasonal deposition of detritus to the deep-sea floor and its subsequent resuspension. *Deep-Sea Research* 32, 885–897.

Martín, J., Miquel, J.C., Khripounoff, A., 2010. Impact of open sea deep convection on sediment remobilization in the western Mediterranean, *Geophys. Res. Lett.,* 37, L13604, doi:10.1029/2010GL043704.

McCave, I.N., 1986. Local and global aspects of the bottom nepheloid layers in the world ocean, *Netherlands Journal of Sea Research*. 20 167-181.

McCave, I.N. and Dickson, R.R., 1986, Nepheloid layers on the continental slope west of Porcupine bank, *Deep-Sea Research* 33, 791-818.

McPhee-Shaw, E.E., Sternberg, R.W., Mullenbach, B., Ogston, A.S., 2004. Observations of intermediate nepheloid layers on the Northern California continental margin. *Cont. Shelf Res*., 24, 693–720.

Ohnemus, D.C., Lam, P.J. Twining, B.S., 2017. Optical observation of particles and responses to particle composition in the GEOTRACES GP16 section. *Marine Chemistry* (2017), http://dx.doi.org/10.1016/j.marchem.2017.09.004

Palanques, A., Martin, J., Puig, P., 2006. Evidence of sediment gravity flows induced by trawling in the Palamós (Fonera) submarine canyon (northwestern Mediterranean). *Deep-Sea Research I*,53: 201-214. DOI: 10.1016/j.dsr.2005.10.003

Penven, P. Lutjeharms, J.R.E., Florenchie, P., 2006. Madagascar: A pacemaker for the Agulhas Current system? *Geophysical Research Letters*. 33 L17609. doi:10.1029/2006GL026854.

Prospero, J.M, and Carlson, T.N., 1981. Sarahan airoutbreaks over the tropical North Atlantic. *Pure Applied Geophysics*, 119, 677-691.

Puig, P., Durrieu de Madron, X., Salat, J., Schroeder, K., Martín, J., Karageorgis, A.P., Palanques, A., Roullier, F., Lopez-Jurado, J.L., Emelianov, M., Moutin, T. Houpert, L., 2013a. Thick bottom nepheloid layers in the western Mediterranean generated by deep dense shelf water cascading. *Progress in Oceanography* 111, 1-23.

Puig, P, Greenan, B.J.W., Li, M.Z., Prescott, R.H., Piper, D.J.W., 2013b. Sediment transport processes at the head of Halibut Canyon, eastern Canada margin: An interplay between internal tides and dense shelf-water cascading. *Marine Geology* 341: 14-28.

Puig, P., Palanques, A., Martın, J. 2014. Contemporary sediment-transport processes in submarine canyons. *Annual Review of Marine Science*, 6(1), 53–77. https://doi.org/10.1146/annurev-marine-010213-135037.

Richardson, M.J., Weatherly, G.L., Gardner, W.D., 1993. Benthic storms in the Argentine Basin. *Deep-Sea Research* 40 975-987.

Richardson, M.J., Wimbush, M., Mayer, L., 1981. Exceptionally strong near-bottom flows on the continental rise of Nova Scotia. *Science* 213, 887-888.

Son, Y.B., Gardner, W.D., Mishonov, A.V., Richardson, M.J., 2009. Multispectral Remote Sensing Algorithms for Particulate Organic Carbon (POC): the Gulf of Mexico, *Remote Sensing of Environment* 113:50–61. DOI: 10.1016/j.rse.2008.08.011.

Thorndike, E.M., 1975. A deep-sea photographic nephelometer. Ocean Eng. 3, 1-15.

Thran, A.C., Dutkiewicz, A., Spence, P.,, Dietmar Müller, R., 2018. Controls on the global distribution of contourite drifts: insights from an eddy resolving ocean model. *Earth and Planetary Science Letters*, 489, 228-240. https://doi:org/10.1016/j.epsl.2018.02.044.

Turnewitsch, R., Falahat, S., Nycander, J., Dale, A., Scott, R.B., Furnival, D., 2013. Deep-sea fluid and sediment dynamics—Influence of hill- to seamount-scale seafloor topography. *Earth-Science Reviews* 127, 203–241.

Van Hulten, M.M.P., Dutay, J.-C. Roy-Barman, M., 2017. Ocean model of Protactinium, Thorium and Particles (ProThorP). https://doi.org/10.5281/zenodo.1009064.

Watts, D.R., Tracey, K.L., Bane, J.M., Shay, T.J., 1995. Gulf Stream path and thermocline structure near 74°W and 68°W. *Journal of Geophysical Research*, Oceans 100, 18,291-18,312.

Wright, C.J., Scott, R.B., Furnival, D., Ailliot, P., Vermet, F., 2013. Global observations of ocean-bottom subinertial current dissipation. *Journal of Physical Oceanography* 43, 402-417. doi: 10.1175/JPO-D-12-082.1

Wunsch, C. Modern Observational Physical Oceanography, Understanding the Global Ocean. Princeton University Press, ISBN. 9780691158822. 512 pp.

Acknowledgements

We thank Lawrence Sullivan and his team for their invaluable expertise in preparing and deploying the Lamont-Thorndike nephelometers, and producing quality E/E_D data from the 52 cruises involved in this work for over >20 years. We also extend thanks to Mary Parsons, Adele Hanley, Adrian Heredia plus other personnel aboard numerous ships, and many colleagues for help in collecting and processing these data. We thank Rebecca Gray Thomas and Kenna Nolen for digitizing the KN74 CTD/Transmissometer data. We thank our students, colleagues and the many technicians on numerous cruises during the last 37 years for their assistance in collecting and analyzing the transmissometer data presented here. Supportive cooperation was provided by many personnel from Ocean Data Facility at Scripps, NOAA personnel, and the many chief scientists during the WOCE, JGOFS, CLIVAR Repeat Hydrography, and GO-SHIP programs. The comments of three anonymous reviewers are greatly appreciated and have helped improve the paper. Synthesis of these data has been supported by: the National Science Foundation (contract OCE-1536565 to Gardner and Richardson), cooperation with CICS-MD/ESSIC/University of Maryland, NCEI/NOAA, and support from the Earl F. Cook Professorship (Gardner). We received funding from NSF for SAVE (OCE-8717231) and JGOFS programs (OCE-9022348, OCE-9310961, OCE-9530837, and OCE-9986762), and from ONR for HEBBLE (N00014-80-C-0098) and for NABE (NOOO14-89-J-1478).

Author Contributions: WDG, MJR and PEB conceived and outlined the analysis and synthesis of the nephelometer parameters. WDG and MJR orchestrated transmissometer data collection, calibrations, and initial analysis. AVM further processed the transmissometer and nephelometer data with QA/QC assistance from WDG and MJR. AVM constructed the figures, interacting with WDG and MJR. WDG wrote the initial manuscript with further development and editing from AVM and MJR.